

Mass Transfer from CO₂ Drops and the Apparent Solubility of CO₂ Under Deep-Ocean Conditions

Yi Zhang^a, Ronald J. Lynn^b, Gerald D. Holder^c
and Robert P. Warzinski^{b*}

^aUniversity of Pittsburgh, Department of Chemical and Petroleum Engineering, 1249 Benedum Hall, Pittsburgh, PA 15261

^bU.S. Department of Energy, National Energy Technology Laboratory, P.O. Box 10940, Pittsburgh, PA 15236

^cUniversity of Pittsburgh, School of Engineering, 240 Benedum Hall, Pittsburgh, PA 15261

*Corresponding Author

ABSTRACT

Understanding the behavior and fate of CO₂ in aqueous systems is important both for developing potential CO₂ sequestration options and for understanding the impacts of seepage or leakage of the stored CO₂ into aqueous environments, such as an unintentional release of CO₂ into the deep ocean from a sub-oceanic sequestration reservoir. To address these important issues, the National Energy Technology Laboratory has developed a unique facility to better understand the behavior of CO₂ in aqueous environments under high pressure. In this device, individual CO₂ drops are observed during suspension in a countercurrent flow of seawater and dissolution rates of the drops are obtained by direct measurement through high-pressure windows. Dissolution rates have been obtained under a range of conditions that include those that exist in the deep ocean down to 3000 m. Similar data were also obtained with elevated levels of dissolved CO₂ in the seawater that simulate the conditions that may occur near a release point. It was observed that stable hydrate shells would form if sufficient dissolved CO₂ was present. A model was developed based on the dissolution rates obtained at different background concentrations of CO₂ that allows calculation of mass transfer coefficients and apparent solubilities of CO₂ at different temperatures and pressures. The impact of different background concentrations on the mass transfer coefficient was also investigated. The model also accounts for the impact of a hydrate coating on the drop. The apparent solubilities obtained from our study were found to be higher than literature data. Utilization of our data for modeling may be desired to predict the fate of CO₂ released into aqueous environments like the deep ocean, since they were obtained under more realistic conditions.

INTRODUCTION

Nonatmospheric sequestration of carbon dioxide is the subject of great national and international concern (Carbon Sequestration, 1999). Large potential sinks include geologic formations, soils and vegetation, and the deep ocean. In both geologic and oceanic systems the CO₂ is often in contact with water, seawater or brines. Understanding the behavior and fate of CO₂ in such aqueous systems is important for developing many of the potential options and for understanding the impacts of seepage or leakage of CO₂ into aqueous environments, such as unintentional release of CO₂ from a sub-oceanic storage reservoir into the deep ocean.

The behavior of CO₂ in water and salt water has been addressed in previous work (Aya, et al.1996; Hirai, et al., 1996a, 1996b; Holder et al., 2001; Mori, et al, 1997; Teng, et al., 1996; Radhakrishnan, et al., 2003; Teng, et al., 1998b). An important issue that impacts research in cold aqueous systems under pressure is the possible formation of the ice-like CO₂ hydrate. The hydrate may be beneficial in that it could potentially seal any unintentional releases from sub-oceanic storage reservoirs as the CO₂ migrates through the cold ocean floor sediments. It could also influence the behavior of any CO₂ that enters the ocean environment at depths below about 500 m. For example, if it forms a thin shell on a CO₂ drop, it could slow the dissolution of the drop. At depths above about 2700 m, this hydrate-encased drop would rise to shallower depths than a drop without a hydrate shell, thus transporting the CO₂ farther up the oceanic water column and likely reducing the time before the CO₂ reenters the atmosphere (Warzinski and Holder, 1999).

While the research mentioned above has greatly contributed to our understanding of the behavior of CO₂ in aqueous systems, there is still some uncertainty with respect to the rates of dissolution and mass transfer associated with a CO₂ drop in an under-saturated aqueous system and on the impact of hydrate on these processes. At the National Energy Technology Laboratory (NETL) a unique device is being used to study the behavior of CO₂ under simulated free rise or free sinking conditions (Warzinski et al., 2004; Haljasmaa et al., 2005). This device, the High-Pressure Water Tunnel Facility (HWTF), is currently being used to measure the rates of dissolution of CO₂ drops and the impact of hydrate at various conditions of temperature, pressure, salinity, and dissolved CO₂.

In this paper, the dissolution rates for CO₂ drops obtained in the HWTF are presented. They are then used to determine mass transfer coefficients for CO₂ drop dissolution in seawater both in the absence and presence of hydrate. By varying the background concentrations of dissolved CO₂, the solubility (or metastable solubility) of liquid CO₂ in seawater has also been determined. This is especially useful when hydrate formation occurs on the surface of a liquid CO₂ drop, which can make the measurement of CO₂ solubility difficult, since the solid phase can be inadvertently mixed and sampled with the aqueous phase. There are limited data on the solubility of CO₂ in seawater (Teng, et al, 1998b; Stewart, et al, 1970) compared to the extensive studies on the solubility of CO₂ in water (Chapoy, et al., 2004; Diamond, et al, 2003; Anderson, 2002; Crovetto, 1991). The present study provides this information under conditions that attempt to simulate the natural behavior of CO₂ as it enters the deep ocean, either through unintentional releases or through an engineered system.

EXPERIMENTAL

The basic operation of the HWTF has been previously described (Warzinski, et al., 2004; Haljasmaa et al., 2005). It basically consists of a flow loop that is used to stabilize a rising or sinking object (bubble, drop or solid particle)in a visual observation section using a countercurrent flow of water and internal flow conditioning elements that prevent the drop from contacting the walls in the device (Warzinski et al., 2000). It also incorporates automated systems for controlling the position of the object in viewing

windows and for measuring and recording the size, shape and motion of the object. Pressures to 34.5 MPa are possible.

The experimental data reported in this paper are for rising CO₂ (99.5% purity) drops suspended in a downward flow of 35 salinity artificial seawater that was prepared following the recipe given by Millero (1996). The same CO₂ was also dissolved into the artificial seawater to prepare solutions of seawater with various levels of dissolved CO₂.

RESULTS

Dissolution data

We have previously presented limited experimental results from the HWTF on the dissolution of CO₂ drops in water (Warzinski et al, 2004) and seawater (Zhang et al., 2004). Here we report additional data for CO₂ drops at simulated depths from 500 m to 2500 m, temperatures from 2°C to 14°C and at dissolved CO₂ concentrations of 0 wt%, 2 wt%, 4 wt% and 4.6 wt%. These data are shown in Figures 1 through 4, respectively. For the data at 0 wt% and 2.0 wt% dissolved CO₂, nearly all of the points in Figures 1 and 2, respectively, are the averages of the results for two or more individual drops. At the higher CO₂ concentrations fewer replicate experiments were performed. The error bars in these Figures represent the standard deviation of the data and in some cases are smaller than the symbol size. The error bars for temperature represent the deviations between individual experiments. Within any given experiment the variations in temperature and pressure are typically less than ±0.1°C and ±0.01 MPa (±2-m depth, respectively).

The dissolution rates generally decrease with decreasing temperature, increasing depth and increasing amounts of dissolved CO₂. No stable hydrate formation was observed except at 2500 m simulated depth and 2.0°C, although hydrate formation is possible at any of these depths at temperatures below 10°C.

The dissolution rate data obtained at 0 wt%, 2 wt%, 4 wt% and 4.6 wt% dissolved CO₂ were fit to first and second order polynomials of the form: $dR/dt = aT^2 + bT + c$. Table 1 gives the values for a , b and c and the sample coefficients of determination. As evidenced in these data, a linear correlation fits the individual data sets for 0 wt%, 2 wt% and 4 wt% very well with nearly all r^2 values greater than 0.98. The data sets at 4.6 wt% were not described as well by a first order polynomial which gave r^2 values for the three shallower depths less than 0.50. Inspection of the 4.6 wt% data shows that even though some curvature of the individual data sets is apparent, all of the dissolution rates are close to 1.5 μmol/cm²s indicating that the effects of pressure and temperature are minimal at this higher level of dissolved CO₂.

Also noteworthy is the fact that the only time a stable hydrate shell formed on a drop was at the highest level of dissolved CO₂. The point in Figure 4 represents the average of three separate drops. The shell on these drops became visibly less thick with time, as evidenced by the change from a rough, translucent shell to a nearly transparent shell in a matter of minutes. While the presence of a hydrate shell may not be discernable from the transparency of the shell, our visual observations show that when a drop with a hydrate shell is present in the HWTF the drop surface is more rigid than in the absence of the shell. That is, it is subject to less distortion (wobbling) by the flow in the HWTF. Hydrate shells, not even transitory ones were observed on any of the drops other than that noted.

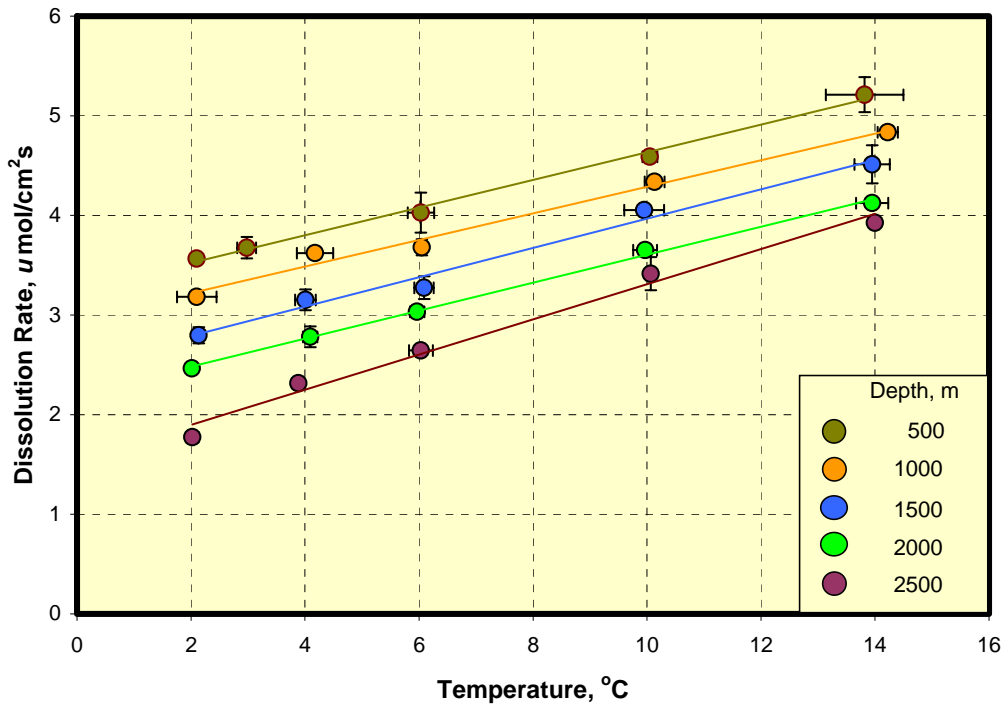


Figure 1. Dissolution rate of CO₂ drops in 35 salinity artificial seawater as a function of temperature and simulated depth with no dissolved CO₂.

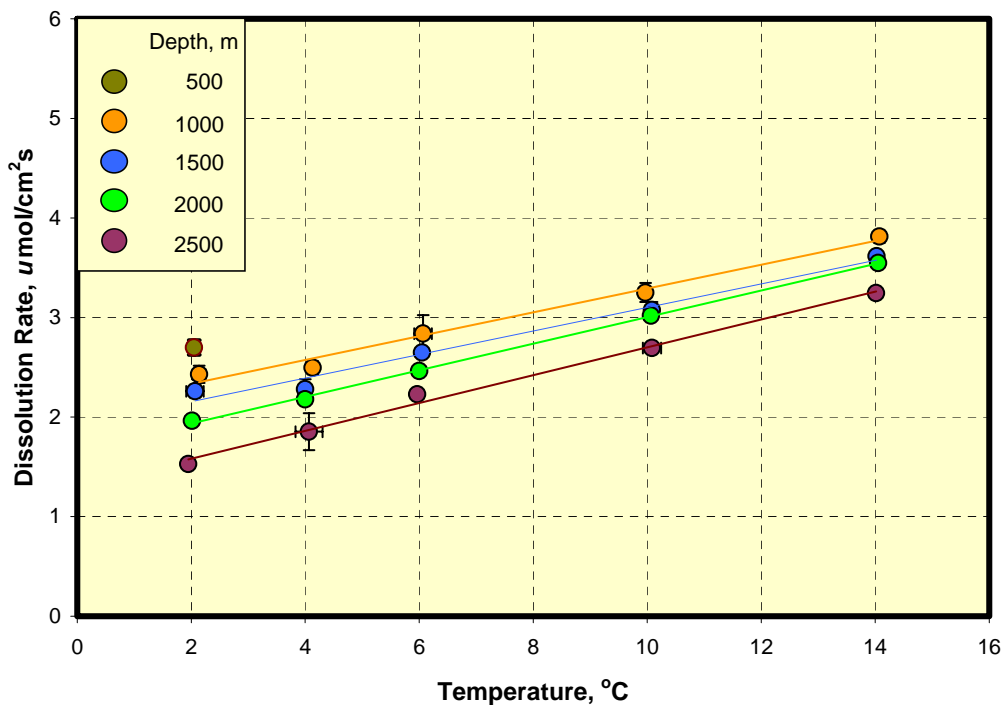


Figure 2. Dissolution rate of CO₂ drops in 35 salinity artificial seawater as a function of temperature and simulated depth with 2 wt% dissolved CO₂.

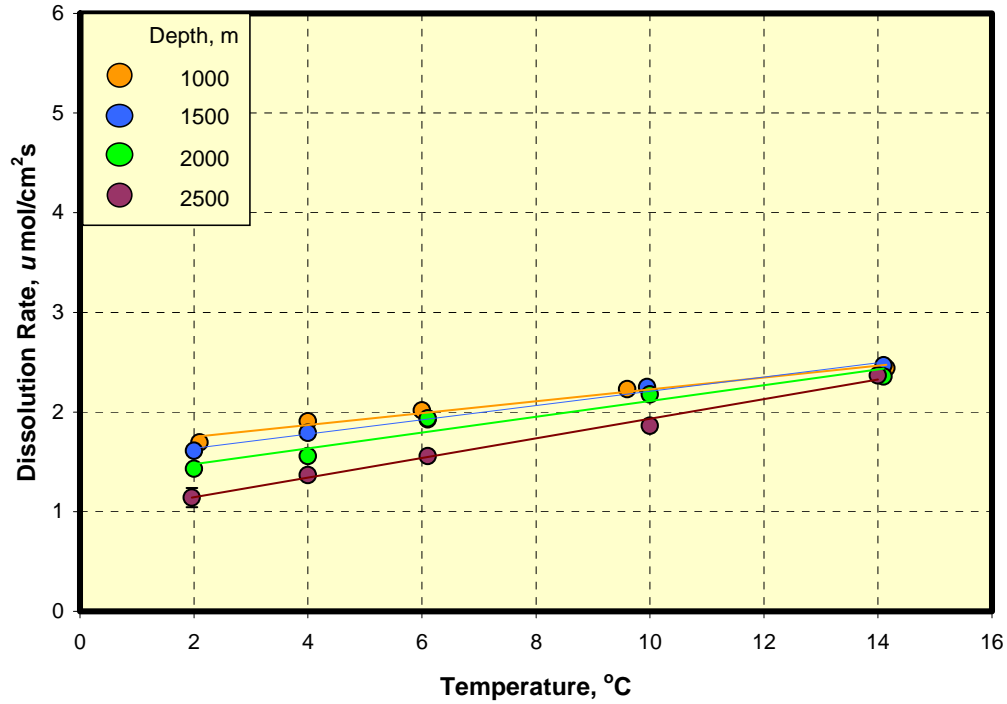


Figure 3. Dissolution rate of CO_2 drops in 35 salinity artificial seawater as a function of temperature and simulated depth with 4 wt% dissolved CO_2 .

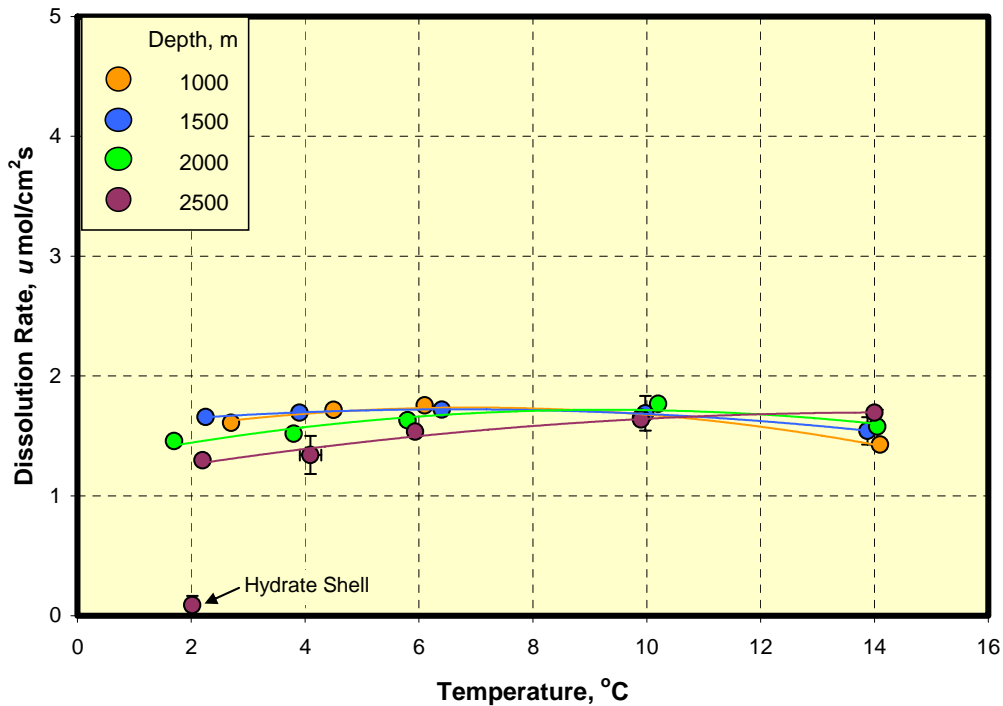


Figure 4. Dissolution rate of CO_2 drops in 35 salinity artificial seawater as a function of temperature and simulated depth with 4.6 wt% dissolved CO_2 .

Table 1. Regression coefficients and correlation coefficients for dissolution rate data.

Depth	a	b	c	r ²
No Dissolved CO₂				
500		0.1389	3.2425	0.9952
1000		0.1334	2.9523	0.9867
1500		0.1471	2.4945	0.9858
2000		0.1404	2.2009	0.9976
2500		0.1767	1.5423	0.9976
2.0 wt% Dissolved CO₂				
1000		0.1196	2.0955	0.9865
1500		0.1182	1.9195	0.9812
2000		0.1335	1.6693	0.9993
2500		0.1400	1.3003	0.9936
4.0 wt% Dissolved CO₂				
1000		0.0595	1.6316	0.9762
1500		0.0715	1.4924	0.9917
2000		0.0792	1.3185	0.9413
2500		0.0984	0.9493	0.9919
4.6 wt% Dissolved CO₂				
1000	0.0062	0.0849	1.4440	0.9680
1500	0.0034	0.0452	1.5719	0.9973
2000	0.0052	0.0961	1.2722	0.8687
2500	0.0029	0.0825	1.1079	0.9584

Determination of Mass Transfer Coefficients and the Solubility of Liquid CO₂ in Seawater

We have developed a method for determining CO₂ solubility and mass transfer coefficients of CO₂ in seawater from the data shown in Figures 1 to 4 (Zhang et al., 2004). In this paper we will illustrate this procedure and a modification of it; however, a more complete presentation will be the subject of a forthcoming journal article that is now being drafted.

The dissolution behavior of the liquid CO₂ droplet is described by Equation (1).

$$\frac{d(\rho_{co_2}V)}{dt} = -kA(C_s - C) \tag{1}$$

Where, ρ_{co_2} is the molar density of liquid CO₂; V and A are the volume and surface area of a liquid CO₂ droplet, respectively. k is the mass transfer coefficient in the boundary layer between the liquid CO₂ and seawater, or between the outer hydrate layer and seawater if hydrates form. C_s is the interfacial concentration of the CO₂, which is the solubility of CO₂ at the system pressure and temperature. When hydrates are not present, C_s is the two-phase solubility where the CO₂ phase can be either gas or liquid. When hydrates are present, C_s is the CO₂ solubility at three-phase equilibrium (VLH) and will be denoted by C_{sh} . C is the ambient concentration of CO₂ in seawater which is sometimes set at non-zero values in the experiments.

For the purposes of this paper, the equivalent spherical diameters of the drops are used in all calculations. Although drop non-sphericity can be an important factor in drop dissolution, in most experiments it was rather close to unity ($0.7 < E < 1$, where $E = \text{height/width of the drop}$). Equation (1) can then be converted into equation (2).

$$\rho_{co2} \frac{dR}{dt} = -k(C_s - C) \quad (2)$$

Hence, the rate of dissolution of a liquid CO₂ droplet can be obtained by measuring its shrinkage rate, dR/dt .

Equation (2) applies whether hydrates are present or not. Hydrate formation does induce a significant change in the rate of the interfacial mass transfer, as subsequent calculations will demonstrate. However, the lower rate of mass transfer is due to the lower solubility of CO₂, C_{sh} , not to a reduction in the mass transfer coefficient as proposed by Teng, et al., 1998a. At a fixed temperature, the dissolution rate is a function of the ambient CO₂ concentration, C , in water, as shown in Equation (2). If we plot the dissolution rate vs. CO₂ concentration, C , at a fixed temperature, the absolute value of the slope should be the mass transfer coefficient k in the boundary layer as indicated in Equation (2). The solubility of CO₂ in water C_s can be calculated from the intercept, which is $-k \times C_s$.

In our previous paper (Zhang, et al., 2004) we described the use of a correlation for mass transfer coefficient given by Cussler, 1997. We have since discovered an error in our earlier work which when corrected resulted in this correlation providing values for k that are five times higher than our experimental values.

We have recently examined another similar correlation by Clift et al., 1978:

$$k = 0.45 \left(\frac{\Delta\rho}{\rho} \right)^{0.3} g^{0.3} \nu^{0.4} d^{-0.1} (Sc)^{-2/3} \quad (3)$$

where k is the mass transfer coefficient; g is the acceleration due to gravity; ν is the kinematic viscosity; d is the drop diameter, $\Delta\rho$ is the density difference between a CO₂ drop and the surrounding fluid; ρ is the

density of the fluid surrounding the drop, and Sc is the Schmidt number defined as $Sc = \frac{\nu}{D_L}$ where D_L is

the diffusion coefficient of CO₂ in seawater. We found that due to the different background concentrations in the experiments, the density of seawater was different, and hence, the flow velocity was also different, which had an impact on the mass transfer coefficient, k . This will be reflected in $\frac{\Delta\rho}{\rho}$,

which is the fractional density difference, and ν , which is the kinematic viscosity of seawater. Note that the correlation for calculating density of CO₂ aqueous solutions given by Teng and Yamasaki, 1998, only applies to certain conditions when the mole fraction of CO₂, x_{CO2} , is the solubility of CO₂ at the given pressure in the seawater. If the seawater is undersaturated as in many of our experiments, the correlation will not provide the correct density. The correlation for calculating the density of seawater with dissolved CO₂ given by Giggenbach (Giggenbach, 1990), which was also used by Fer and Haugan (Fer and Haugan, 2003), was used in this paper. The density of seawater without dissolved CO₂, which was required in the

correlation, was obtained by the UNESCO equation of state (UNESCO, 1981). An online program was used to obtain the value from the UNESCO equation of state (Kelley, 2003). Viscosities of seawater containing various CO₂ concentrations were obtained by correcting the viscosities of aqueous solutions (Kumagai and Yokoyama, 1998) to those of seawater solutions. Linear correlations between mole fractions of CO₂ in aqueous solutions and viscosity were developed. The viscosity of the aqueous solution when the mole fraction of CO₂ in aqueous solution was zero, which was the viscosity of water, was substituted by the viscosity of seawater (Chemical Hazards Response Information System, 1999), assuming that mole fraction of CO₂ has the same impact on viscosity of seawater solution as that of water. The temperature dependence of the diffusivity, D_L , of CO₂ in seawater is based on the assumption that it varies by $\frac{D_L \mu}{T} \cong \text{constant}$, where μ is the absolute viscosity of the seawater, as suggested in Perry's Chemical Engineers' Handbook (Perry, 1997). D_L is 1.9×10^{-5} cm/s at 1 bar, 24 °C in seawater (Millero, 1996).

For the condition of our study, density and kinematic viscosity change, but $\frac{k}{\left(\frac{\Delta\rho}{\rho}\right)^{0.3} \nu^{-0.267}} \cong$ should be

constant at a fixed temperature based upon Equation (3). Our original model (Equation 2) was modified as follows to include the effect of density and viscosity change on the mass transfer coefficients. This modified model enables prediction of mass transfer coefficients at different background concentrations of dissolved CO₂ at a given temperature and pressure, which can be compared with the values obtained from the correlations.

$$\rho_{CO_2} \frac{dR}{dt} = - \frac{k}{\left(\frac{\Delta\rho}{\rho}\right)^{0.3} \nu^{-0.267}} \left[\left(\frac{\Delta\rho}{\rho}\right)^{0.3} \nu^{-0.267} (C_s - C) \right] = -K (C_s' - C) \quad (4)$$

where $\frac{k}{\left(\frac{\Delta\rho}{\rho}\right)^{0.3} \nu^{-0.267}} = K \quad (4a)$

$$\left(\frac{\Delta\rho}{\rho}\right)^{0.3} \nu^{-0.267} C_s = C_s' \quad (4b)$$

and $\left(\frac{\Delta\rho}{\rho}\right)^{0.3} \nu^{-0.267} C = C' \quad (4c)$

While k will vary from condition to condition, K should remain essentially constant at a given temperature and pressure. When the dissolution rate is plotted versus C' , the slope will be K , which is the mass transfer coefficient corrected by the density and viscosity effect. The actual mass transfer

coefficient, k , can be obtained from $k = \left(\frac{\Delta\rho}{\rho}\right)^{0.3} \nu^{-0.267} * K$ at any condition. The intercept, $K C_s'$, divided by K and $\left(\frac{\Delta\rho}{\rho}\right)^{0.3} \nu^{-0.267}$, will give the estimation of the solubility of CO_2 , C_s , in seawater.

Because we have data with different background concentrations of dissolved CO_2 , we can use this data to determine mass transfer coefficients and CO_2 solubility in aqueous solutions by applying the above method. An example, using the experimental data collected at 25 MPa is shown below. In these experiments, a seawater velocity in the range of 6 cm/s to 13 cm/s was required to stabilize the droplets in the viewing section of the HWTF.

Figure 5 depicts dissolution rates calculated from the regression equations shown in Table 1 as a function of corrected concentration of CO_2 , C' , for the experimental data at 25 MPa. The dissolution rates were calculated at seven different temperatures (14°C , 12°C , 10°C , 8°C , 6°C , 4°C , 2°C) for the four different levels of dissolved CO_2 used (0 wt%, 2 wt%, 4 wt%, 4.6 wt%). A straight line fit of the data is adequate.

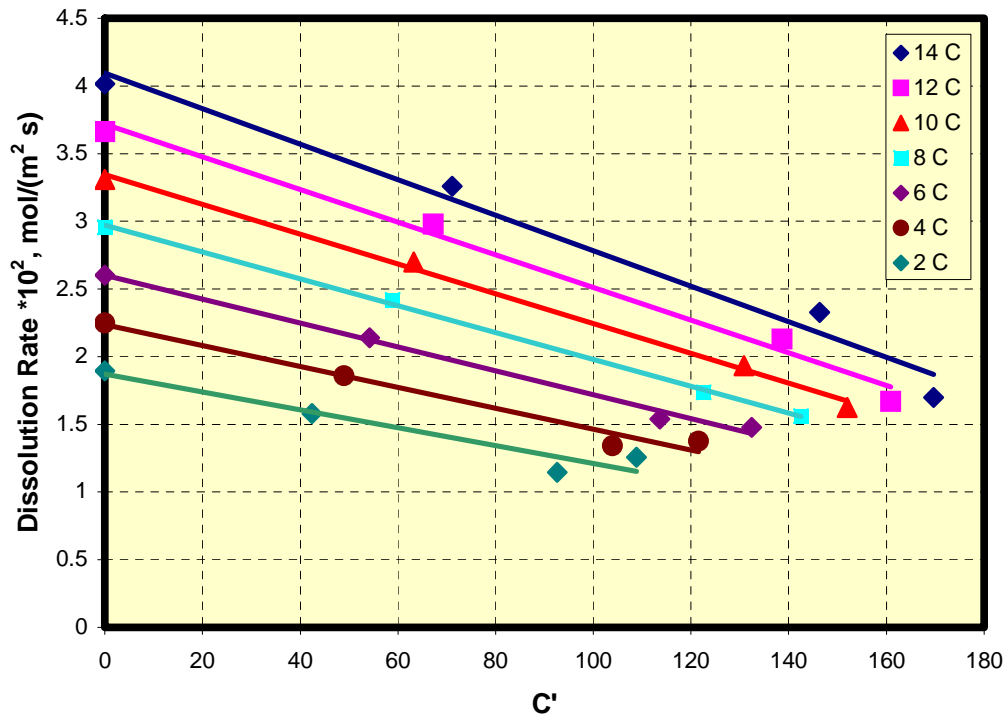


Figure 5. Dissolution rate, $\rho_{\text{CO}_2}(dR/dt)$, as a function of corrected CO_2 concentration, C' , at different temperatures at 25 MPa

By using the method described above, the solubilities of CO_2 in seawater, C_s , and the mass transfer coefficients, k , were determined as functions of temperature for a simulated depth of 2500 m (25 MPa). The results are shown in Figures 6 and 7, respectively. Also shown are calculated results for the solubility of CO_2 , C_{sh} , and k when hydrates were present. Note that some of the solubilities are the

solubility of CO₂ in a metastable state since some temperatures and pressures were at conditions where hydrates can form but did not. As can be seen from the Figure 6, the presence of hydrate decreased the solubility of CO₂ in the surrounding seawater dramatically. This is an actual equilibrium solubility. In general, hydrates did not form because the bulk solution was undersaturated with CO₂. The only place where the reported solubilities actually exist is at or near the interface. Also note that the mass transfer coefficient when hydrate was present is also shown in Figure 7 by the solid circle. The procedure for obtaining this value is described in the next section.

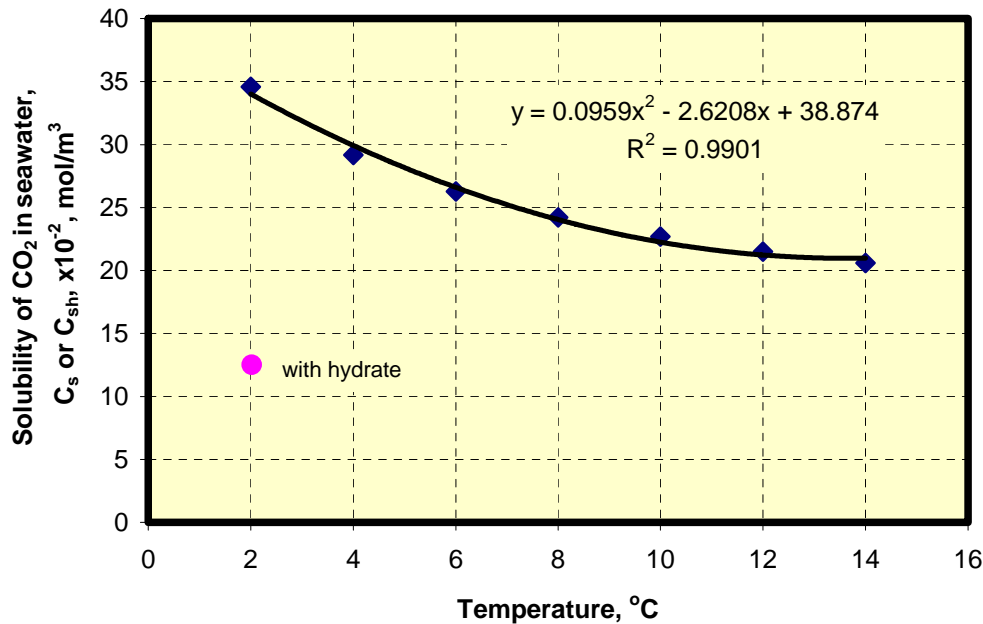


Figure 6. Solubility of CO₂, C_s or C_{sh} , in seawater as a function of temperature at 25 MPa from our experiments.

The determination of the solubility of CO₂ when hydrates were present, as shown in Figure 6, requires further explanation. We assume that the water adjacent to the drop is saturated with carbon dioxide. When the hydrates are absent, this saturation is the (metastable) solubility of liquid CO₂ at the system pressure. When the hydrates are present, the solubility is the three-phase (VLH) solubility. If the concentration was any higher, more hydrate would form from the supersaturated water. Thus the driving force is $C_{sh} - C$ when hydrates are present and $C_s - C$ when they are absent. However, the mass transfer is limited by the water phase and the mass transfer *coefficient* should be the same whether hydrates are present or not.

Using the correlation for CO₂ solubility, C_s , developed in Figure 6, the dissolution rate at 2°C as a function of the corrected driving force when hydrates were absent, $\left(\frac{\Delta\rho}{\rho}\right)^{0.3} \nu^{-0.267} (C_s - C)$, at 0 wt%, 2 wt% and 4 wt% of background concentrations is plotted in Figure 8. A linear correlation is shown. The

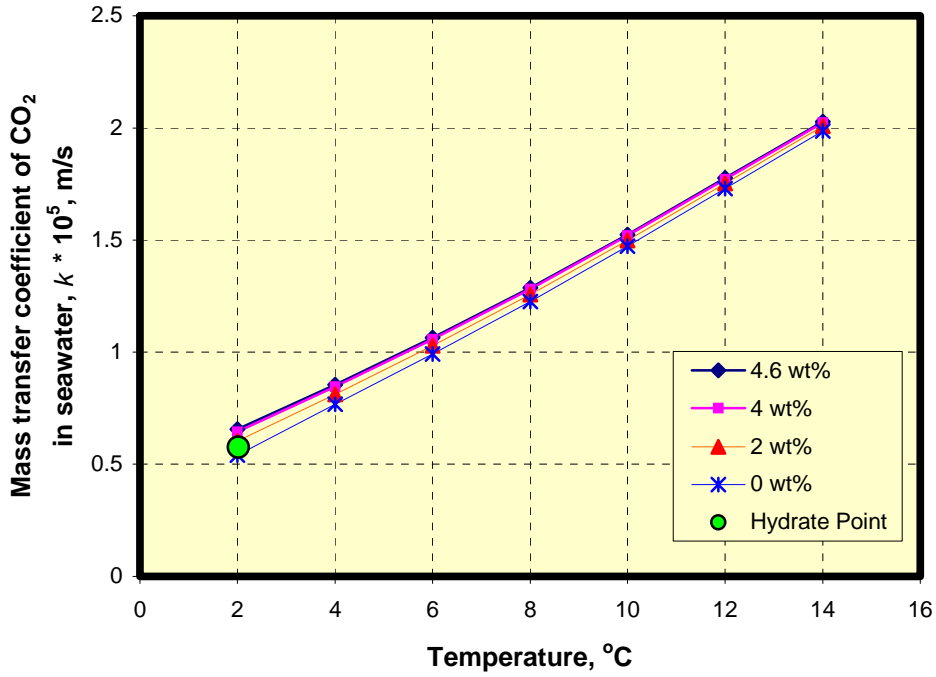


Figure 7. Mass transfer coefficient, k , under different background concentrations as a function of temperature in seawater at 25 MPa from our experiments.

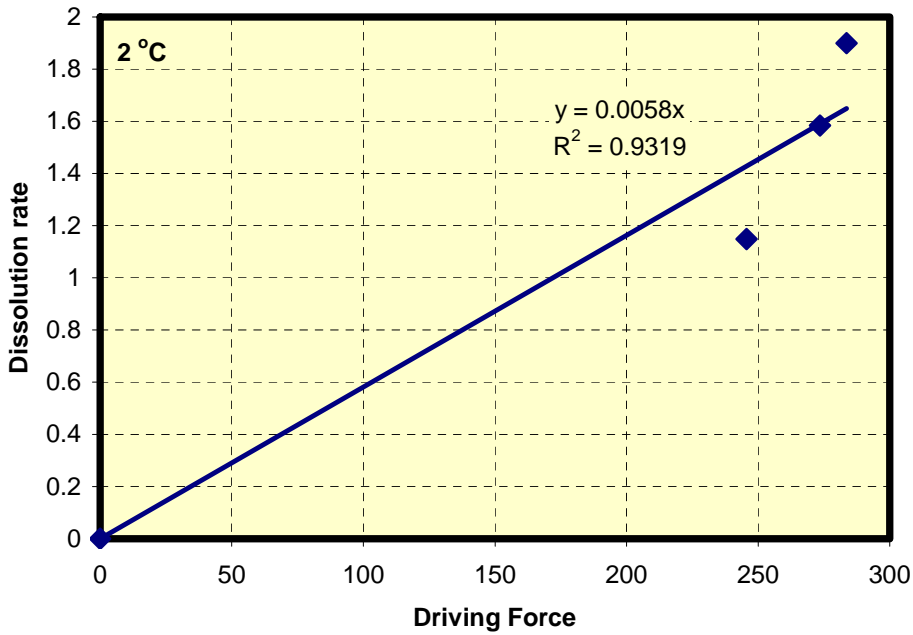


Figure 8. Rate of dissolution, $\rho_{CO_2}(dR/dt)$, as a function of driving force at 2°C at 25 MPa.

slope of this correlation is the mass transfer coefficient, K , at this temperature with or without the presence of hydrate shell. The mass transfer coefficient at 4.6 wt%, k , was obtained by multiplying K by $\left(\frac{\Delta\rho}{\rho}\right)^{0.3} \nu^{-0.267}$. Using this k and the experimentally measured dissolution rate in the presence of hydrate, C_{sh} is obtained from the following equation and shown by the solid circle in Figure 6.

$$\rho_{co2} \frac{dR}{dt} = -k(C_{sh} - C) \quad (5)$$

To test the validity of using the value of K obtained when hydrates were not present to obtain the k when hydrates were present, we compared our three-phase solubility (1251 moles/m³) to that calculated using the method of Diamond and Akinfiyev (2003), which gives a value of 984 moles/m³. The close agreement supports the use of one value of k whether or not hydrates are present.

DISCUSSION

The mass transfer coefficients obtained from the data obtained in the simulated deep-ocean conditions in the HWTF are two orders of magnitude larger than those obtained in the static system used by Teng, et al., 1998a. It has previously been shown that even a small flow of 0.3 cm/s can cause a factor of 10 increase in the value of k (Radhakrishnan, et al., 2003). Also, in our experiments, a small (typically 0.7 cm diameter or less) CO₂ drop was injected into a large volume of circulating seawater (16.4 L). Under these conditions the ambient concentration of CO₂ was nearly constant as the drop dissolved. In contrast, the system used by Teng et al., 1998b had a volume of 0.07 L and the concentration of the CO₂ in water column changed as the CO₂ dissolved. In our previous work in a static 0.04 L cell, the observed dissolution rates were also lower (Warzinski et al., 1997). From a design perspective, the mass transfer coefficients reported here are those expected when CO₂ droplets move under their own buoyancy in a large volume of seawater.

We have also compared the mass transfer coefficients determined from our experimental data with those obtained from the correlation of Clift et al., 1978 (Equation 3). The results are shown in Figure 9. The agreement is much better than that previously found when using the correlation of Cussler, 1997, as previously mentioned. We are currently working on a modification of the correlation of Clift et al., 1978 that further improves the agreement.

Finally, Figure 10 compares our solubility results with the values determined by Teng et al., 1998b. The disagreement is larger than would be expected. Ohmura and Mori (1999) suggest that Teng's solubilities may be low. Our values are also higher than those obtained in fresh water (Diamond, 2003), which we did not show here. We think what we obtained are apparent solubilities, not true solubilities of CO₂ in seawater, and the difference reflects the limitation of the models as described below. However, the apparent solubilities we obtained will be more useful for design purposes, because they will yield more accurate estimation of dissolution rates.

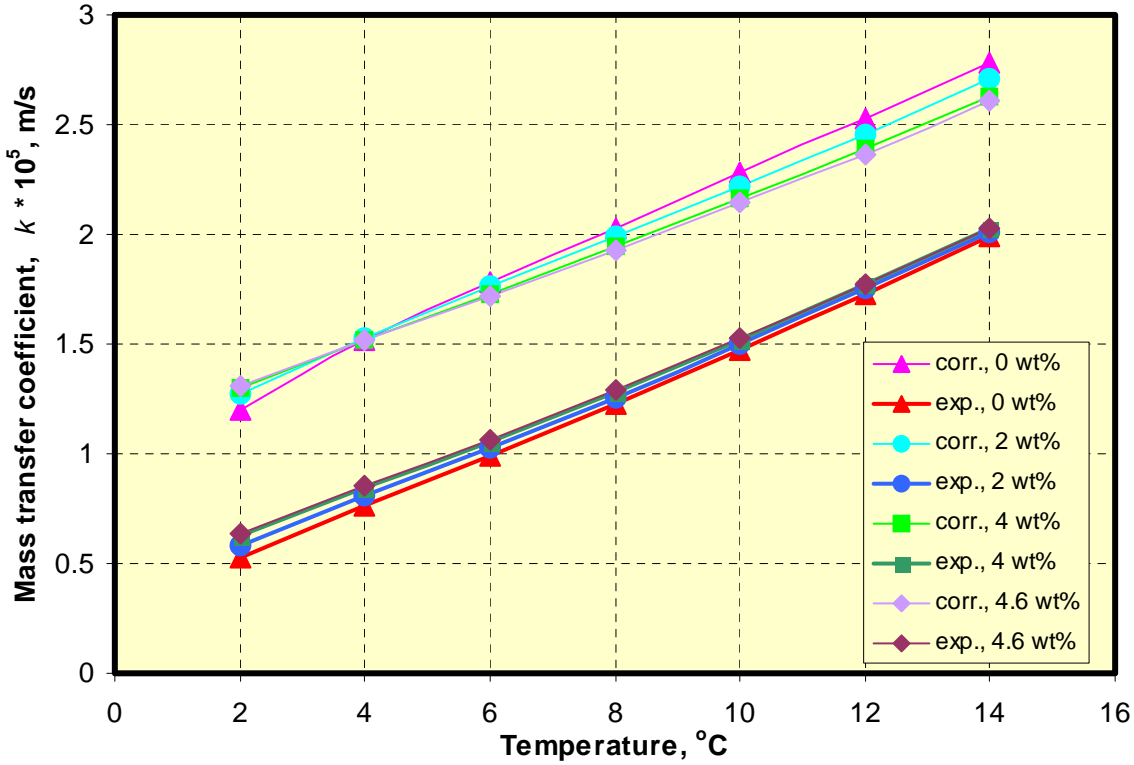


Figure 9. Comparison of our results and calculated results on mass transfer coefficient, k , of CO_2 in seawater under different background concentrations at 25 MPa.

The possible reason for obtaining higher solubility is the following: the mass transfer coefficient changes in a non-linear way as the concentration approaches saturation. Our method, which applies when the dissolution rate is proportional to concentration difference, is approximate in that situation. Diffusion flux is proportional to the chemical potential gradient,

$$-j_1 = \frac{D_0 c_1}{k_B T} \nabla \mu_1 = \left[D_0 \left(1 + \frac{\partial \ln \gamma_1}{\partial \ln x_1} \right) \right] \nabla C_1, \quad (6)$$

which will lead to $D = D_0 \left(1 + \frac{\partial \ln \gamma_1}{\partial \ln x_1} \right)$ (Cussler, 1997). Applying the four-suffix Margules equation (Prausnitz, et al, 1997):

$$\ln \gamma_1 = \alpha_2 x_2^2 + \alpha_3 x_2^3 + \alpha_4 x_2^4 \quad (7)$$

to the equation of diffusion coefficient, becomes:

$$D = D_0 (1 - (1 - x_2)(2\alpha_2 x_2 + 3\alpha_3 x_2^2 + 4\alpha_4 x_2^3)), \quad (8)$$

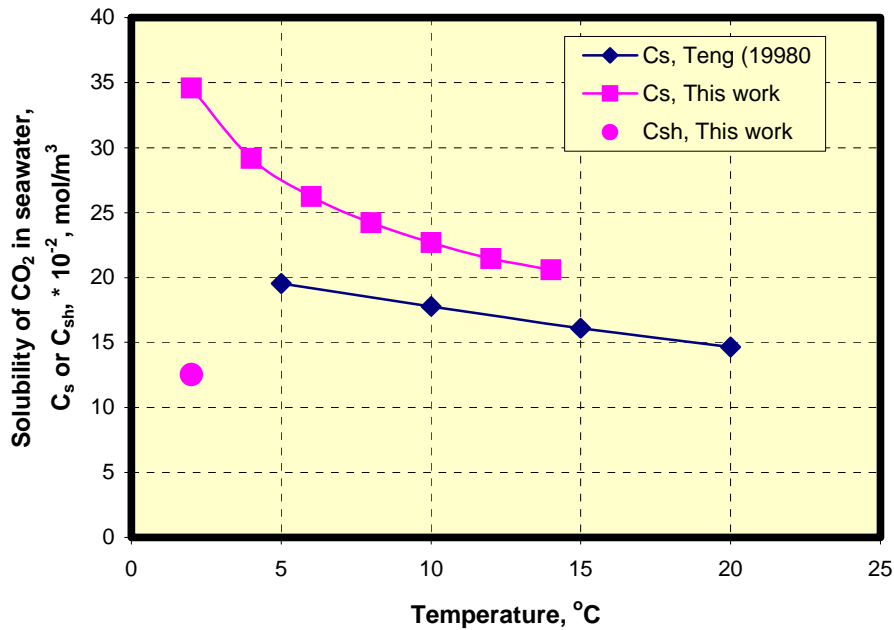


Figure 10. Comparison of our results with the data of Teng et al., (1998b), on the solubility of CO₂ in seawater at 25 MPa.

where the diffusion coefficient, D_0 , is corrected by the activity coefficient, and $\alpha_2, \alpha_3, \alpha_4$ are parameters fitted from experimental activity coefficient data. The above derivation shows that the diffusion coefficient, D , is a function of concentration and it changes with concentration in a non-linear way, which indicates that the mass transfer coefficient can also behave in a similar way, especially at higher concentrations.

Summary

Dissolution rates of CO₂ in seawater under simulated deep ocean situation were reported. A model was developed to obtain the mass transfer coefficients and solubilities of CO₂ in seawater. The study shows that the model can give fairly good prediction of mass transfer coefficients, however, the apparent solubility obtained is higher than true solubility. For design purposes, the solubilities estimated here are needed for calculation of dissolution rates at design conditions.

REFERENCES

- Anderson, G. K. "Solubility of carbon dioxide in water under incipient clathrate formation conditions," *J. Chem. Eng. Data* **2002**, 47, 219-222.
- Aya, I.; Yamane, K.; Narai, H. "Solubility of CO₂ and density of CO₂ hydrate at 30 MPa," *Energy* **1996**, 22, 263-271.
- Carbon Sequestration, Research and Development*, U.S. Department of Energy Report, DOE/SC/FE-1, 1999, OSTI, Identifier Number 810722 at www.osti.gov/bridge.
- Chapoy, A.; Mohammadi, A. H.; Chareton, A.; Tohidi, B.; Richon, D. "Measurement and modeling of gas solubility and literature review of the properties for the carbon dioxide- water system," *Ind. Eng. Chem. Res.* **2004**, 43, 1794-1802.



CONFERENCE PROCEEDINGS

- Chemical Hazards Response Information System (CHRIS), March 1999,
<http://www.chrismanual.com/Intro/prop.htm>.
- Clift, R.; Grace, J. R.; Weber, M. E. *Bubbles, Drops, and Particles*; Academic: New York, 1978; p 125.
- Crovetto, R., "Evaluation of solubility data for the system CO₂- H₂O from 273 K to the critical point of water," *J. Phys. Chem. Ref. Data* **1991**, 20 575-589.
- Cussler, E. L. *Diffusion: mass transfer in fluid systems*, 2nd ed.; 1997, Cambridge University: London, 1997; pp 224-225.
- Demurov, A.; Radhakrishnan, R.; Trout, B. L. "Computations of diffusivities in ice and CO₂ clathrate hydrates via molecular dynamics and Monte Carlo simulations," *J. Chem. Phys* **2002**, 116, 2:702-709.
- Diamond, L.W.; Akinfiev, N. N. "Solubility of CO₂ in water from -1.5 to 100 °C and from 0.1 to 100 MPa: evaluation of literature data and thermodynamic modeling," *Fluid Phase Equilibria* **2003**, 208, 265-290.
- Fer, I.; Haugan, P. M. "Dissolution from a liquid CO₂ lake disposed in the deep ocean", *Limnol. Oceanogr.* **2003**, 48(2), 872-883.
- Giggenbach, W. F. "Water and gas chemistry of Lake Nyos and its bearing on the eruptive process". *J. Volcanol. Geotherm. Res.* **1990**, 42, 337-362.
- Haljasmaa, I. V.; Vipperman, J. S.; Lynn, R. J.; Warzinski, R. P. "Control of a fluid particle under simulated deep-ocean conditions in a high-pressure water tunnel," *Review of Scientific Instruments* **2005**, 76, 025111.
- Hirai, S.; Okazaki, K.; Araki, N.; Yoshimoto, K.; Ito, H.; Hijikata, K. "Experiments for dynamic behavior of carbon dioxide in deep sea," *Energy Convers. Mgmt.* **1996a**, 36, 471-474.
- Hirai, S.; Okazaki, K.; Araki, N.; Yazawa, H.; Ito, H.; Hijikata, K. "Transport phenomena of liquid CO₂ in pressurized water with clathrate-hydrate at the interface," *Energy Convers. Mgmt.* **1996b**, 37, 1073-1078.
- Holder, G. D.; Mokka, L. P.; Warzinski, R. P. "Formation of gas hydrates from single-phase aqueous solutions," *Chem. Eng. Sci.* **2001**, 56, 6897-6903.
- Kelley, D., 2003, UNESCO equation of state,
<http://www.phys.ocean.dal.ca/~kelley/seawater/density.html>.
- Kumagai, A. and Yokoyama, C. "Viscosity of aqueous solutions of CO₂ at high pressures," *Int. J. Thermophysics*, **1998**, 19, 1316-1323.
- Millero, F. J. *Chemical Oceanography*, 2nd Ed.; CRC: Boca Raton, Florida, 1996; 67.
- Mori, Y. H.; Mochizuki, T. "Dissolution of liquid CO₂ into water at high pressures: A search for the mechanism of dissolution being retarded through hydrate-film formation," *Energy Convers. Mgmt.* **1997**, 39, 567-578.
- Ogasawara, K.; Yamasaki, A.; Teng, H. "Mass transfer from CO₂ drops traveling in high-pressure and low-temperature water," *Energy & Fuels*, **2001**, 15, 147-150.
- Ohmura, R.; Mori, Y. H. "Comments on 'Solubility of liquid CO₂ in synthetic seawater at temperatures from 278K to 293K and pressures from 6.44 MPa to 29.49 MPa, and densities of the corresponding aqueous solutions,'" (Teng, H.; Yamasaki, A., *J. Chem. Eng. Data*, **1998**, 43, 2-5), *J. Chem. Eng. Data*, **1999**, 44, 1432-1433.
- Perry, R. H.; Green, D. W.; Maloney, J. O. *Perry's Chemical Engineers' Handbook*, 7th ed.; McGraw-Hill: New York, 1997; p 2-330.
- Radhakrishnan, R.; Demurov, A.; Herzog, H.; Trout, B. "A consistent and verifiable macroscopic model for the dissolution of liquid CO₂ in water under hydrate forming conditions," *Energy Convers. Mgmt.* **2003**, 44, 771-780.
- Stewart, P. B., Munjal, P. "Solubility of carbon dioxide in pure water, and synthetic seawater concentrates at -5° to 25°C and 10 to 45 atm pressure," *J. Chem. Eng. Data* **1970**, 15, 67-71.

CONFERENCE PROCEEDINGS

- Teng, H.; Yamasaki, A. "Mass transfer of CO₂ through liquid CO₂-water interface," *Int. J. Heat and Mass Transfer* **1998a**, *41*, 4315-4325.
- Teng, H.; Yamasaki, A. "Solubility of liquid CO₂ in synthetic seawater at temperatures from 278 K to 293 K and pressures from 6.44 MPa to 29.49 MPa and densities of the corresponding aqueous solutions," *J. Chem. Eng. Data* **1998b**, *43*, 2-5.
- Teng, H.; Yamasaki, A.; Shindo, Y. "Stability of the hydrate layer formed on the surface of a CO₂ droplet in high-pressure, low-temperature water," *Chem. Eng. Sci.* **1996**, *51*, 4979-4986.
- UNESCO "Tenth report of the Joint panel on oceanographic tables and standards"; *Technical Report in Marine Science No. 36*, 1981; UNESCO, Paris, 25 pp.
- Warzinski, R. P.; Holder, G. D. "The effect of CO₂ clathrate hydrate on deep-ocean sequestration of CO₂," *Proc., 9th Int. Conf. on Coal Science*, Ziegler, A.; van Heek, K. H.; Klein, J.; Wanzl, W., eds., Vol. III, **1997**, P & W Druck and Verlag GmbH, Essen, Germany, 1879-1882.
- Warzinski, R. P.; Holder, G. D. "Ocean storage of CO₂: Experimental Observations of clathrate hydrates in seawater," in *Greenhouse Gas Control Technologies*, Eliasson, B.; Riemer, P.W.F.; Wokaun, A., eds., Pergamon, Amsterdam, **1999**, 237-242.
- Warzinski, R. P.; Lynn, R. J.; Robertson, A. M.; Haljasmaa, I. V. "Development of a high-pressure water tunnel facility for ocean CO₂ storage experimentation," *Prepr. Pap., Amer. Chem. Soc., Div. Fuel Chem.* **2000**, *45*, 809-813.
- Warzinski, R. P.; Lynn, R. J.; Haljasmaa, I. V.; Zhang, Y.; Holder, G. D. "Dissolution of CO₂ drops and CO₂ hydrate stability under simulated deep ocean conditions in a high-pressure water tunnel," *Proc., 3rd Annual Conf. on Carbon Sequestration* **2004**, Alexandria, Virginia.
- Zhang, Y.; Warzinski, R. P.; Lynn, R. J.; Holder, G. D. "Mass Transfer Coefficient and Solubility of CO₂ Drops and CO₂ Hydrates under Simulated Deep Ocean Situations," Record of Presentation, 2004 AIChE Annual Meeting, Austin, Texas, paper 381f.